

## **Groundwater Aquifer Delineation Within Some Parts Of Olabisi Onabanjo University, Southwestern Nigeria, Using Combined Electrical Resistivity And Magnetic Methods**

\* <sup>1</sup>Coker, J.O., <sup>1</sup>Oladunjoye, H.I., <sup>2</sup>Olasunkanmi, N.K., <sup>3</sup>Ikhane, P.R. <sup>1</sup>Adenuga, O.A. and <sup>1</sup>Adekoya, S.A.

<sup>1</sup>Department of Physics, Olabisi Onabanjo University Ago –Iwoye Ogun State, Nigeria

<sup>2</sup>Department of Physics and Materials Science, Kwara State University, Malete, Nigeria

<sup>3</sup>Department of Earth Sciences, Olabisi Onabanjo University Ago-Iwoye, Ogun State, Nigeria

---

### **Abstract**

Geophysical method is a major tool in groundwater exploration. Integrated geophysical investigations were carried out within the premises of the Olabisi Onabanjo University hostel to delineate the aquifer characteristics of the area. For this study, Vertical Electrical Sounding (VES) configuration was used to unravel the subsurface litho-stratigraphic information of the area. The overburden thickness vis-a-vis the direction of fractured and weathered rock formations was obtained through the acquisition of magnetic data. Five geophysical traverses were established with seven VES points within the study area. The apparent resistivity data acquired from the Electrical Resistivity method was processed, inverted, and iterated using "WinResist". The ground magnetic data were processed using SignProc and Euler deconvolution for the estimation of the depth to bedrock and direction of the fractured lineament. From the results, the residual magnetic anomalies (RMA) has an amplitude range within -185.18 – 269.53 nT. The value of the magnetic data after the Gaussian correction shows a value ranging from -4.8 nT to 3.9 nT. Three (3) geo-electrical layers were delineated representing the topsoil, clay, and fractured/ weathered/ fresh basement. The second geo-electric layer comprising of mainly clayey formations are described with average resistivity values loitering between 30.2 – 80.4  $\Omega$ m with average thickness values of 3.7 and 6.4 m. VES1 and VES5 show the proximity of producing high groundwater yield with the presence of weathered and fractured basement in the points. Consequently, profile 1 of the magnetic data showed the presence of high overburden thickness which serves as a good signature for the presence of high groundwater potential.

**Keywords:** Aquifer., Groundwater yield., Residual magnetic anomalies., Vertical Electrical Sounding.

---

Date of Submission: 02-12-2020

Date of Acceptance: 17-12-2020

---

### **I. Introduction**

Groundwater is water found beneath the earth's surface, occupying the cracks and crevices of the rock. The location of the groundwater contributed to its purity devoid of major contamination/pollution [1, 2]. The primary source of groundwater is precipitation from rain and snow, which falls and then seeps into the ground. As a result of this, groundwater is the largest available source of freshwater in which its contamination depends mainly on the litho-stratigraphic units that harbor the aquifer [3]. The soil and rock type are one of the factors that define the nature and characteristics of the aquifer. When an aquifer is surrounded by permeable sediments, recharge and discharge process will be easy compared to aquifer bordered by impermeable formation. Other factors that influence the recharge rate of an aquifer are climate, land slope, and vegetation [4].

The global distribution of water indicates that groundwater is about 60 times as much as freshwater in lakes or rivers on the surface of the ground [5,6]. The quest for water for domestic and industrial purposes has drifted humanity from ordinary search for surface water to groundwater through the sinking of boreholes of varying grades. The rapid increases for the searches of groundwater have resulted from rapid industrialization, population growth, agricultural-related activities (such as irrigation farming, fishing, and poultry activities). Although with the support of exploration geophysics and the advent of technology, the ratio of a failed borehole (borehole with no/low yield) has reduced.

The identification of lithological formations harboring groundwater usually has several physical attributes which can be deciphered through various geophysical techniques such as electrical resistivity, seismic, magnetic methods, etc. The groundwater is explored through the estimation of the related parameters of the subsurface which are determined by the geophysical methods. Previous researches by [7, 8] have shown the efficacy and efficiency of different configurations of electrical resistivity in exploring groundwater. The

lithologic units with groundwater are usually depicted through the processed apparent resistivity values. Therefore, the 2D resistivity technique portrayed a better resolution of the subsurface identifying the fractured and weathered part of rock fragments. The estimation of the thickness of overburden materials is best determined through magnetic methods [9, 10]. Studies have shown the usefulness and effectiveness of this method in determining the orientation and direction of fracture on the basement [11, 12].

Previous studies have shown that the exploration of groundwater in basement involves the studies of the geology composition of the area concerning for weathering history, nature and depth of weathered layer, groundwater flow system, vis-a-vis with the recharge and discharge techniques [13, 14]. [15] affirmed that decrease in the reflection coefficient and relatively high overburden thickness enhances the productivity of boreholes in major areas of the basement terrain, therefore, good research of groundwater potential will consider overburden thickness, reflection coefficient and presence of fractures as cursory measures in determining the high yield aquifer in basement complex.

Therefore, the integration of the two geophysical techniques tends to yield accurate results via the location and determination of the weathered and fractured components of the aquifer for drilling. Besides, it is expected that the results obtained from this study would generate detailed groundwater conditions. Likewise, it will explicate the groundwater yielding capacity of each point, to reduce waste of resources on points with low yield. Certainly, this will solve the quest for the water by the students living in the hostel and the future builders that intend to construct engineering structures in the area. Besides, the contribution to knowledge and the development of the campus might have been achieved through scientific research.

## II. Materials and Methods

### Location and Geology of the Area of Study

The geology of Nigeria, as detailed in [16] comprises of three primary rock groups which are mainly basement crystalline metamorphic-igneous-volcanic rocks; quaternary alluvial deposits, mesozoic to tertiary sediments and granites and volcanic [17, 18]. The Precambrian Basement rocks consist of migmatite, banded gneisses and granite gneisses, with metasedimentary and metavolcanicschists low grade, intruded by charnockites and Pan-African age granites. The area of study falls within the basement terrain of Nigeria (Figure 1).

The basement terrain is one of the three major litho-petro logic units that make up Nigeria geology. Four (4) different types of rocks were delineated in the study area. These rocks are porphyroblastic gneiss, quartzite schist, banded gneiss and hornblende-biotite granite [19, 20]. The formations of these rocks are mainly gneiss family of the metamorphic rocks. The porphyroblastic gneiss comprises of uncompleted foliated rocks, which forms the larger phenocryst that are aligned in the same direction but not completely stretched. The quartzite schist is a metamorphic formation with main composition of mostly quartz with some mica and tourmaline. This formation constitutes a good aquifer in basement complex due to its geological composition. The banded gneiss and hornblende-biotite granite are formations/rocks rich in quartz, biotite and other accessory minerals. They are mainly foliated rocks with bands of dark and light coloured minerals. Minor rock types found to be active in the study area include pegmatite and quartz veins.

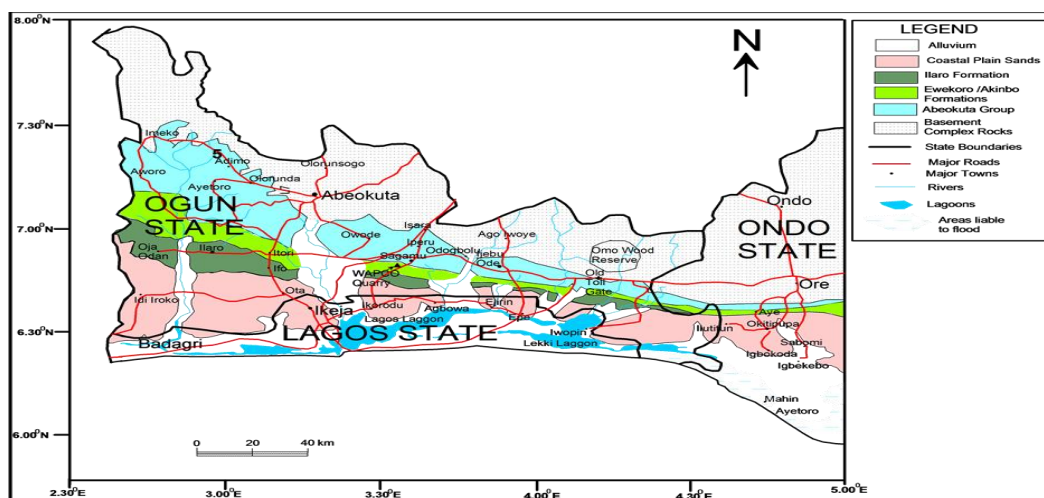


Figure 1: Geological map of Ogun state, Nigeria [16].

### Accessibility of the Study Area

The study was carried out within the main campus premises of Olabisi Onabanjo University, Ago – Iwoye. The location of the study area lies between the Latitudes of  $6.942344^{\circ}$  -  $6.942282^{\circ}$ N and Longitudes of  $3.921332^{\circ}$  -  $3.921426^{\circ}$ E. The study area was accessible through minor road links linking the points to the proposed second gate of the Campus. The data acquisition locations were positioned a few kilometers away from the OOU venture hostel to avoid inherent noise as a result of domestic tools. The remote location of the study area is represented in figure 2 as extracted from google maps. The location is relatively flat with no steep slope.

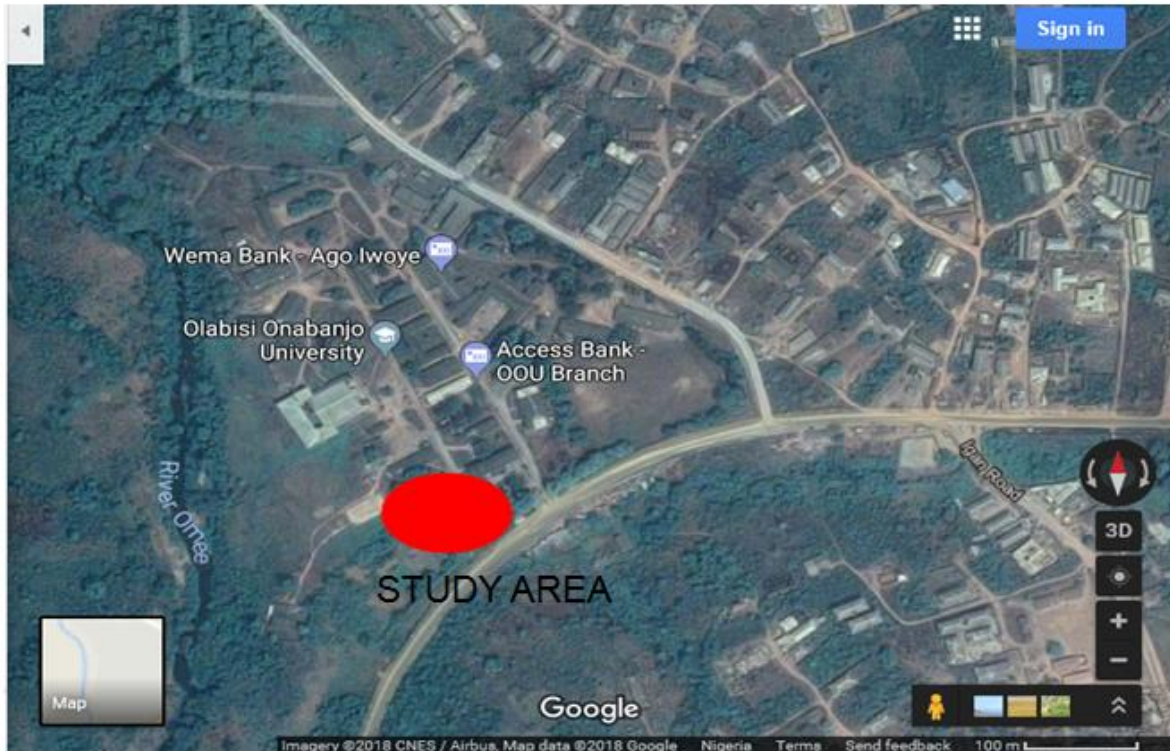


Figure 2: Accessibility map of the study Area google (google map.com)

### III. Magnetic Data Methodology

The GEM 19T proton precession magnetometer was employed for the acquisition of the Total Magnetic Intensity (TMI) of the study area. It is a highly sensitive advanced magnetometer with a precision of 0.1nT. It consists of a control unit box, 2m long sensor rod, coil engulfed kerosene sensor cylinder, and the sensor connector. The kerosene sensor contains hydrogen dipoles enriched with free unpaired electrons. The basic working principle of the magnetometer is that the current is passing through the coil and is made to generate a magnetic field ( $B_p$ ) with a magnitude of 50 – 100 times greater than the natural Earth's Magnetic field in a different direction (Figure 3). This process will make the protons to realign in the new direction. Consequently, the protons return to their original alignment by spiraling or precessing's, in phase around this direction with a period (T) of about 0.5 ms to achieve their original orientation.

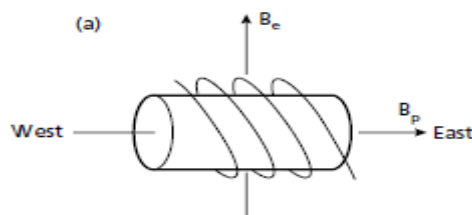
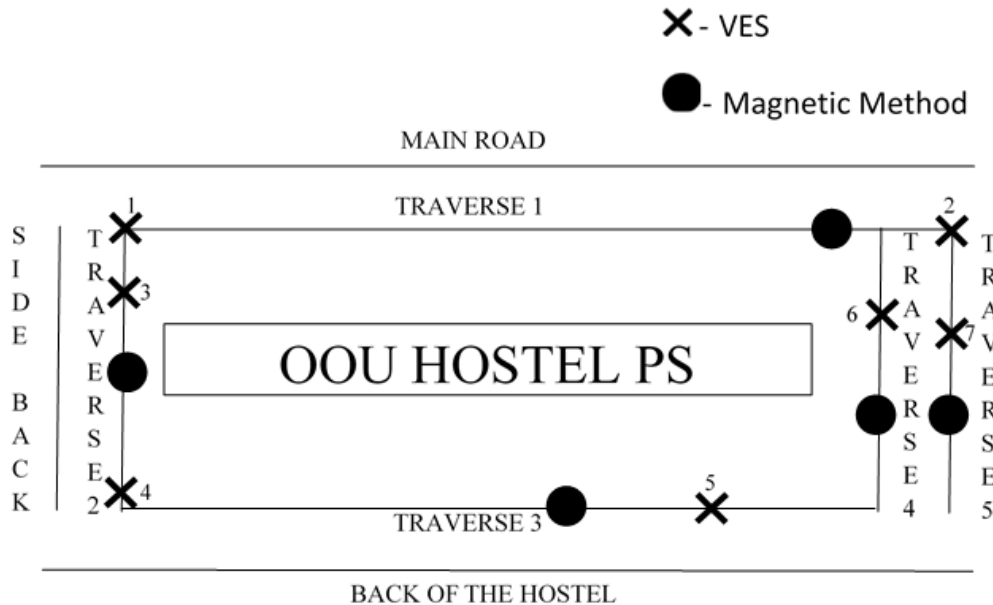


Figure 3: Principle of proton precession magnetometer [21]

To acquire data with less noise ratio, detailed physical scrutiny of the operator and his crew along with the study area was carried out. The survey areas were made to be devoid of metallic objects or structures that can distort the local magnetic field during the acquisition exercise. The diurnal variations within the Earth's

magnetic field were monitored from the selected base stations where the magnetic intensities were measured at a still (stationary) points. The gridding of the survey area was carried out using the Cartesian coordinate system with the station interval of 5 m equidistant to each other. The (base) reading was taken with the time of reading at one of the base stations. The Magnetometer was then moved to the next point on the grid for the acquisition of its Total Magnetic Intensity (TMI) reading. This procedure was painstakingly and progressively followed throughout the gridded points in the survey area repeated measurements at the base stations of each traverses to keep the track of the temporal changes (diurnal changes) in the Earth's magnetic field. Five (5) traverses were strategically established diagonally to one another (Figure 4), only traverse 4 and 5 were placed parallel to each other with an inter-traverse spacing of 20 m.



**Figure 4:** Data acquisition base map showing the distribution of the data points around the study location.

Then, to improve the data quality and production of anomaly maps; upward continuations, analytic signal amplitude (ASA), and total derivative maps were developed. The RMI was upwardly continued to a height of 3 m, 5 m, 8 m, and 12 m to attenuate the high-frequency anomalies, which reveals deeper sources [22, 23] that could be observed at 1.5 m, 2.5 m, 4 m, and 6 m depths. An analytic signal was used to establish the contacts of magnetic bodies as its amplitude (ASA) peaks over magnetic contacts [24] while the total derivative helped to normalize the signatures in images of the magnetic data which makes the structures (i.e., fractures, faults, etc.) conspicuous [25]. Depths to magnetic sources were estimated from Euler solution at spectral indices  $N = 0$  for contacts,  $N = 1$  for intrusive bodies, and  $N = 2$  for a linear source (line of dipoles or poles, and a homogeneous cylinder, rod, etc.) respectively [26]. The eventual magnetic data were presented as magnetic profiles by plotting the magnetic values against station separations for each traverse. Magnetic contour map (2D plot) and surface map (3D plot) of Analytic Signal Amplitude were also constructed for more qualitative interpretation using Surfer 8 software.

The Schlumberger configurations were employed to carry out the sounding procedure using Vertical Electric Sounding (VES) techniques. The arrangement of the four (4) electrodes in this array was made in such a way that (Figure 5), the two outer electrodes provide the energy while the two inner electrodes receive the potential from the ground. The potential electrodes are installed at the center of the electrode array with a small separation, typically less than one-fifth of the spacing between the current electrodes. During the survey, the current electrodes are changes progressively to a higher separation while the potential of electrodes are not changing until the observed voltage value cannot be measured. Typically, expanding the current electrodes occurs roughly six times per survey. The choice of this configuration includes good resolution, higher probing depth, and small time-consuming during the field exercise.

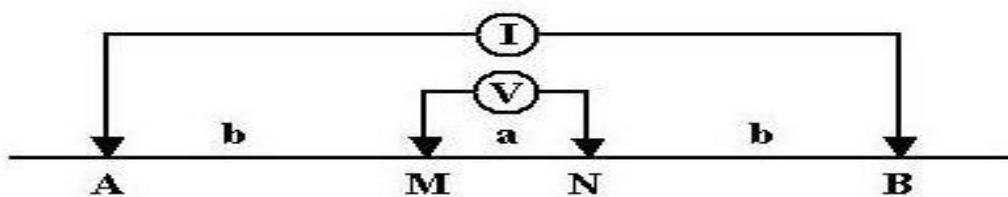


**Figure 5:** Schematic representation of the configuration employed in the study [21].

The data acquisition procedure was accomplished using ABEM Terrameter SAS 1000 with its accessories. The accessories include the four (4) stainless electrodes, hammer, electrode cable, battery, and electrode clips. Seven (7) VES stations were acquired along the established five (5) traverses shown in figure 4. The apparent resistivity values were estimated through the multiplication of the measured resistance values with the geometric factor. The processed data were plotted on the bi-log graph with apparent resistivity values ( $\rho_a$ ) on the ordinate while the current separation is plotted on the abscissa. The curve generated were processed quantitatively using special curves of partial curve matching to generate layered apparent resistivity with their corresponding thickness. The curves were further iterated using computer software called “WINRESIST”.

#### IV. Results and Discussion

##### Magnetic Data Results

The residual magnetic anomalies (RMA) along with each profile (Figure 6) revealed the amplitude range within -185.18 – 269.53 nT with transverse 1 having the highest distribution (Figure 6a) while transverse 4 (Figure 6d) traverses has the least magnetic intensity variation.

The TMI and RMA maps (figure 7) show the contrasting lithologic formation with a strong correlation in pattern and trend of anomalies. The low magnetic anomalies are depicted with blue-purple for magnetic intensity range around -60 to -180 nT, attributable to the intrusion of weakly magnetic rocks which are normally polarized at contact with more highly magnetic rocks depicted with yellow-red for magnetic intensity range around 100 – 269 nT and conspicuous at the north – northeast, south and western region of the area. The intermediate magnetic anomalies range within -10 to +10 depicted with dark – light green and show distinctly the rock-rock boundaries or fracture/fault.

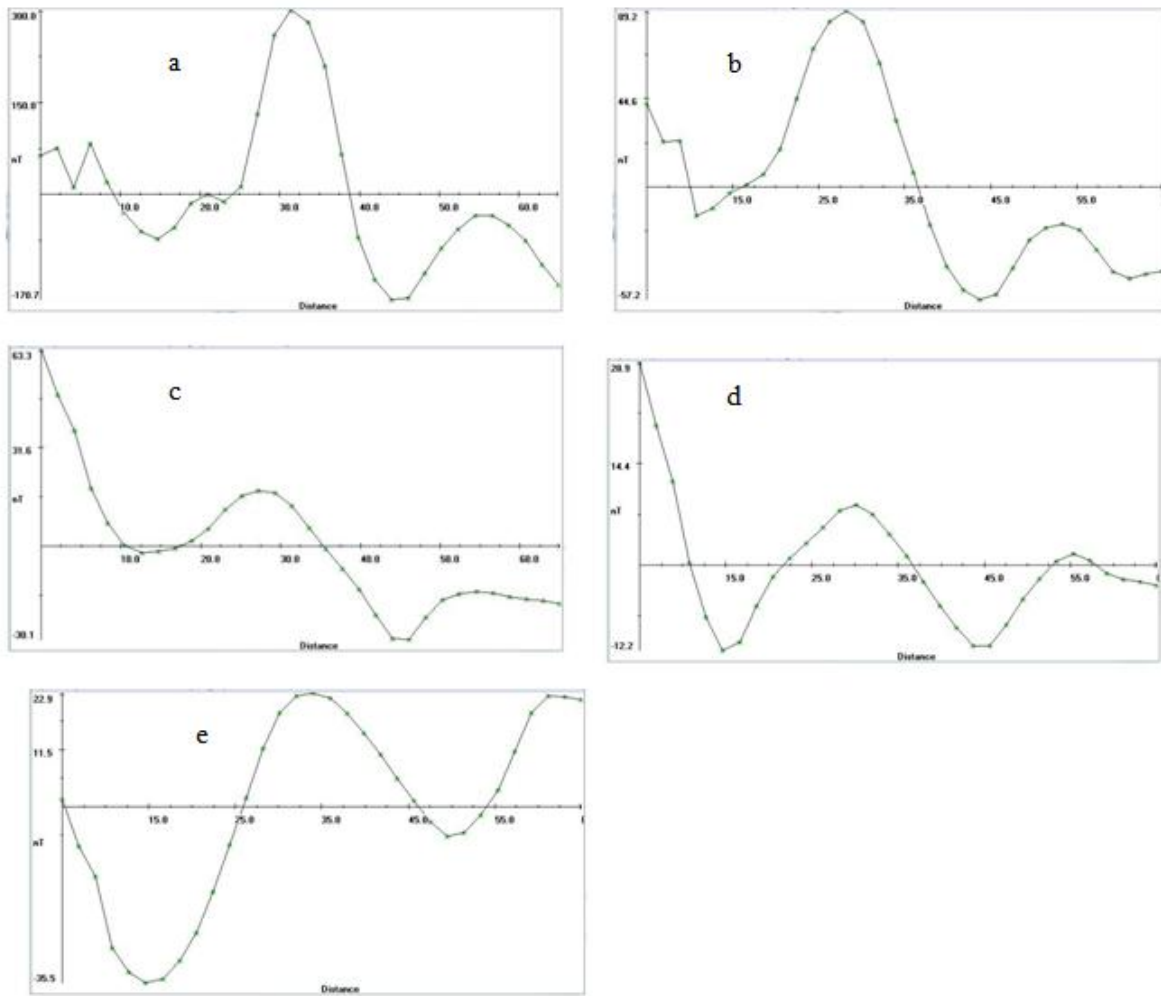


Figure 6: Residual Magnetic anomalies along (a) to (e) i.e Transverse 1 to 5

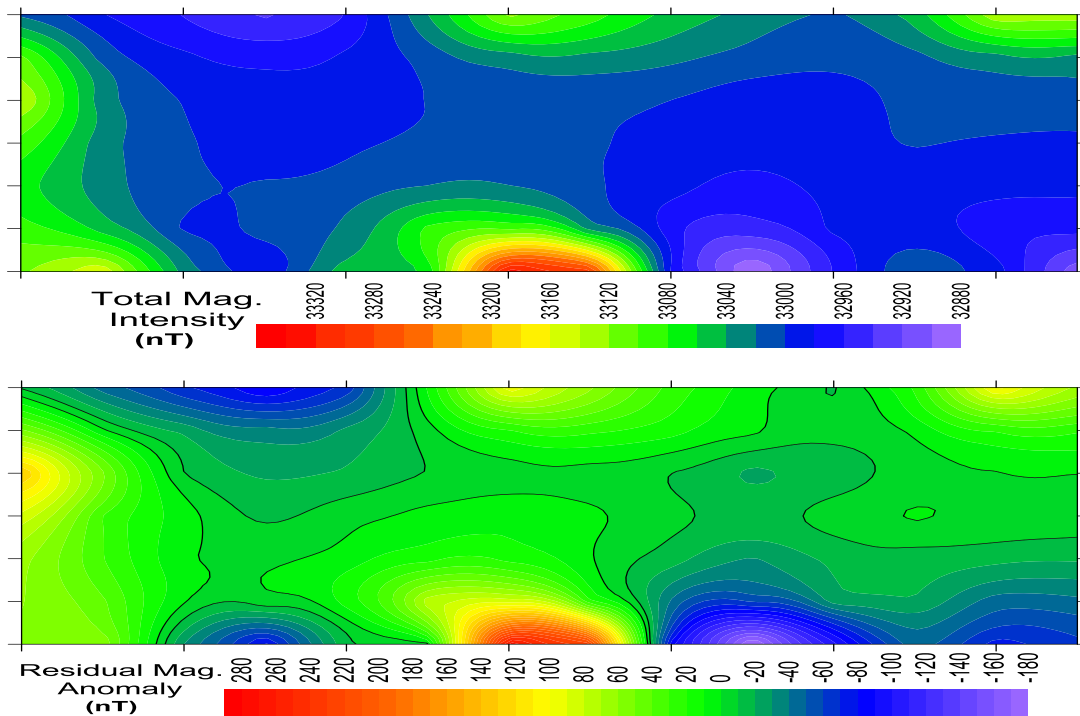
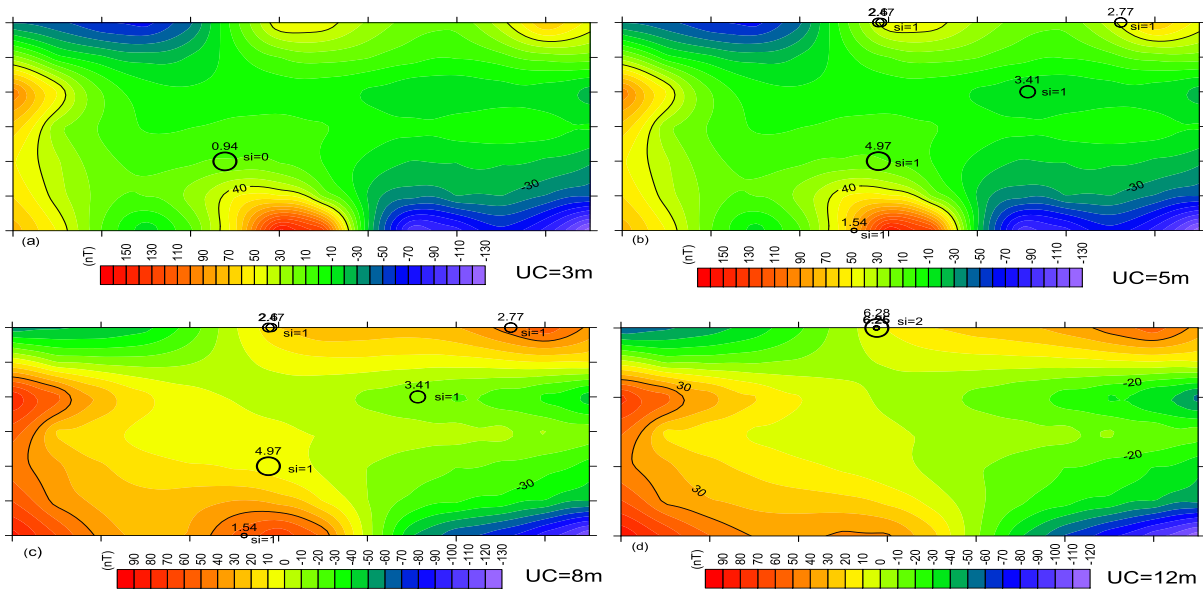
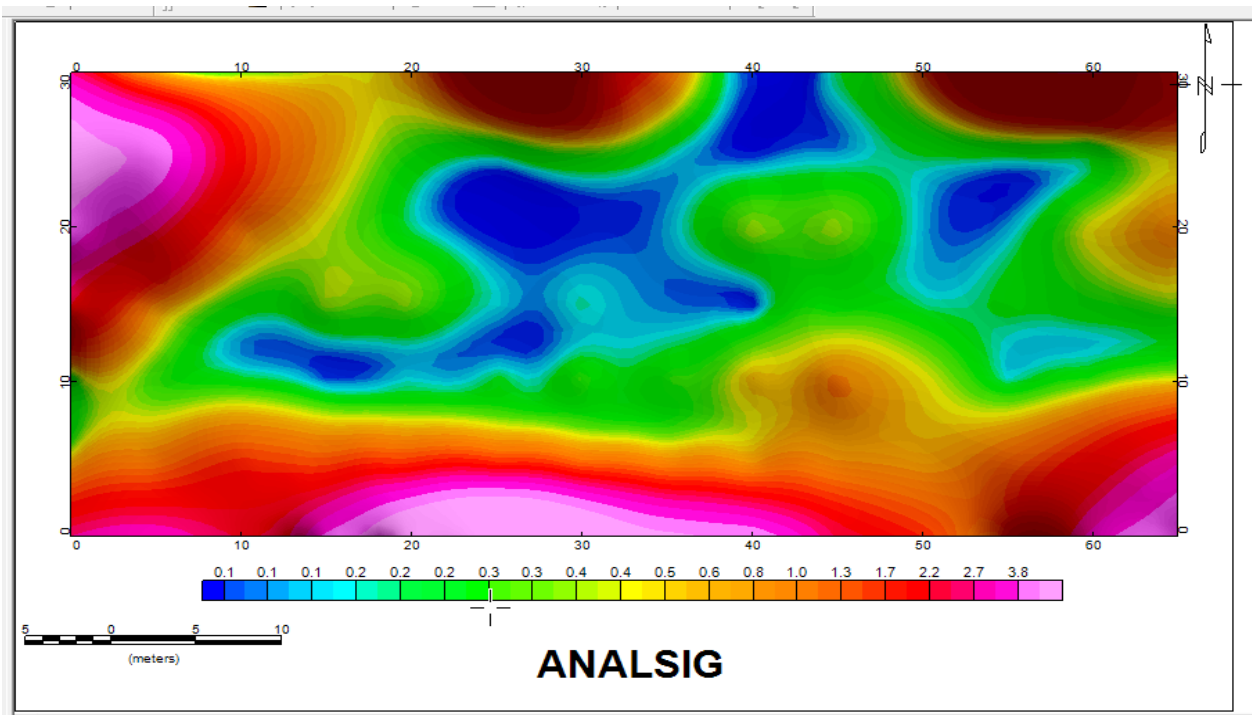


Figure 7: (a) Total Magnetic Intensity Map (b) Residual Magnetic Anomaly Map

The signature of the rock intrusion is corroborated with the increasing amplitude of vertical continuation to depth range 1.5 – 6 m (Figure 8) and the high analytic signal amplitude (ASA) (Figure 9). The region of low ASA correspond areas with deeper depth to bedrock which is evident on the Euler deconvolution map (Figure 10).



**Figure 8:** Vertical continuation of residual magnetic anomalies to heights of (a) 3 m (b) 5 m (c) 8 m (d) 12 m.



**Figure 9:** Analytic Signal Amplitude Map

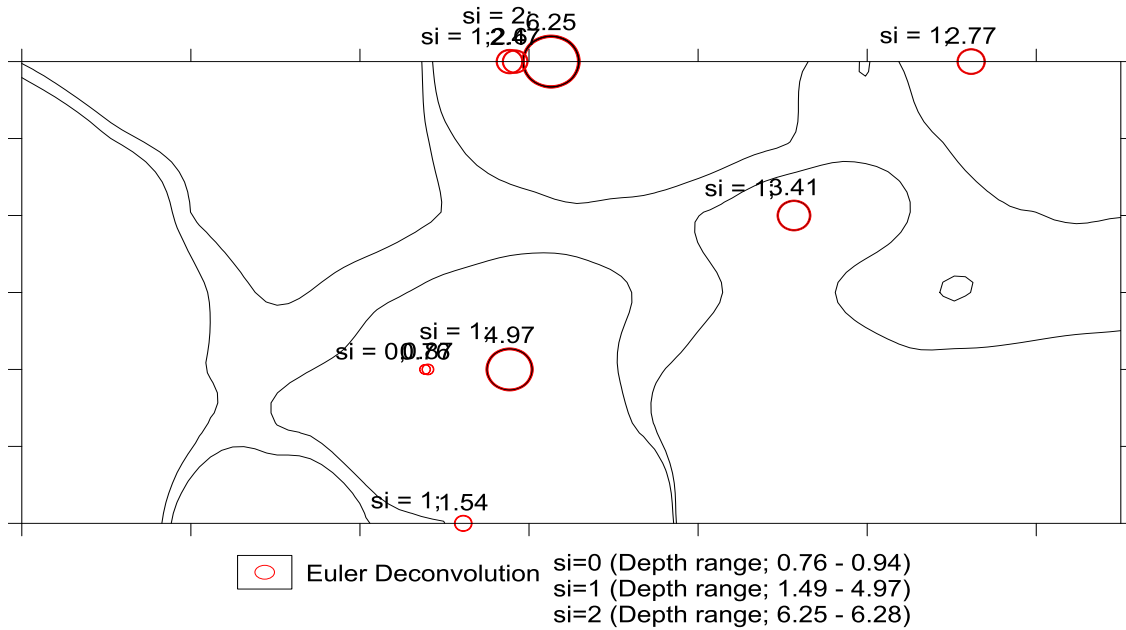


**Figure 10:** Euler plot at  $s_i = 0, 1, 2$

The Euler map depicts a notable contact in the south, using structural index  $N = 0$  with an estimated depth range 0.8 – 0.9 m. The intrusive bodies are depicted with  $N = 1$  at depth range 1.5 - 5 m and are suspected as a homogeneous cylinder (using the  $N = 2$ ) in the north at deeper depth of 6.3 m. Some fractures (lineaments) were revealed within the southern and northwestern parts of the area (Figure 11).

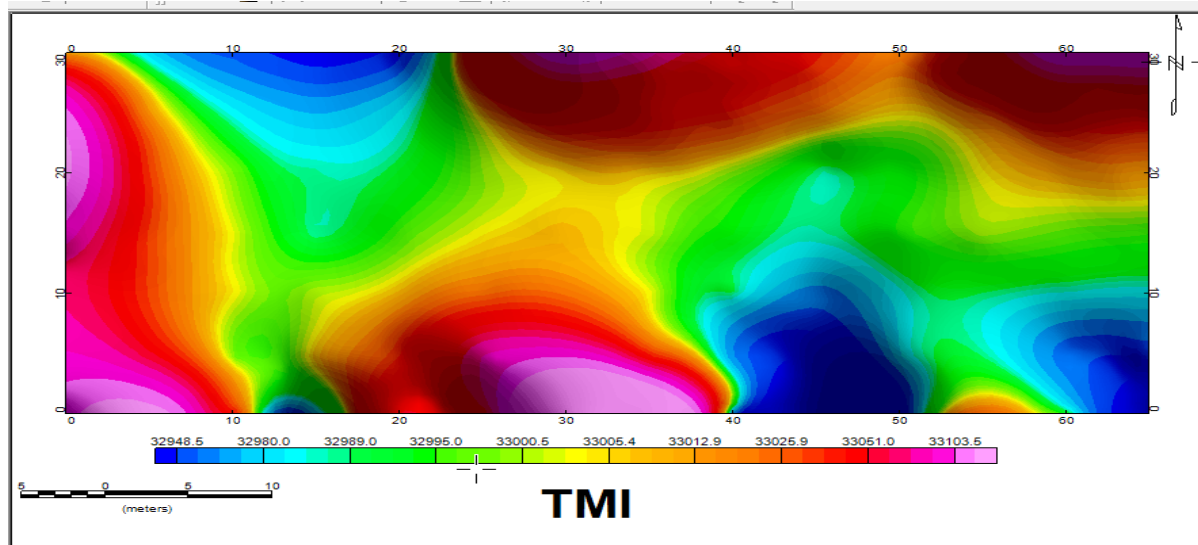


**Figure 11:** TMI Map

### Results of Vertical Electrical Sounding (VES) in the study area

The results of the VES data were presented in an iterative form (figure 12a - g) and its qualitative representation (Table 1). The iterative representation shows the apparent resistivity of each delineated layer with its corresponding thickness. The qualitative representation gives the inferred lithological arrangement based on the outlined resistivity values as described by [27]. The seven (7) VES points obtained in the study area unraveled three (3) layers of geo-electric consisting of topsoil, clayey layer, and weathered/fractured/fresh basement.



**Table 1:** Summary of geo-electric layers parameters in the area of study.

VES No	No of Layers	Resistivity (Ohm-m)	Thickness (m)	Depth (m)	Lithology	Curve Types
1	1	380.0	0.8	0.8	Topsoil	H
	2	80.4	4.7	5.5	Clay	
	3	660.2	-	-	Fractured basement	
2	1	242.0	1.2	1.2	Topsoil	H
	2	40.9	2.6	3.7	Clay	
	3	1199.1	-	-	Fresh basement	
3	1	78.9	1.8	1.8	Topsoil	H
	2	69.0	4.6	6.4	Clay	
	3	1259.6	-	-	Fresh basement	
4	1	200.5	1.7	1.7	Topsoil	H
	2	36.0	3.3	4.9	Clay	
	3	1629.2	-	-	Fresh basement	
5	1	138.3	1.9	1.9	Topsoil	H
	2	67.3	2.4	3.1	Clay	
	3	972.3	-	-	Fractured basement	
6	1	184.4	1.1	1.1	Topsoil	H
	2	54.6	4.4	5.5	Clay	
	3	2818.7	-	-	Fresh basement	
7	1	413.6	2.1	2.1	Topsoil	H
	2	30.2	2.4	4.5	Clay	
	3	6746.8	-	-	Fresh basement	

The 1-D results of VES1 showed three (3) layers of lithology comprising of topsoil, clayey layer, and fractured basement. The topsoil is characterized by the value of resistivity 380.0  $\Omega$ m and thickness 0.8 m. The second geo-electric layer resistivity is 80.4  $\Omega$ m with a thickness of 4.7 m. This layer is indicative of the clayey layer. The third layer with a resistivity value of 660.2  $\Omega$ m describing fractured basement layer with an infinite thickness. Similarly, in VES5 the topsoil has a resistivity value of 138.3  $\Omega$ m with a thickness value of 1.9 m. The clayey layer found in this point is characterized with a resistivity value of 67.3  $\Omega$ m with a thickness value of 2.4 m. The fractured basement delineated in this VES points is described with a resistivity value of 972.3  $\Omega$ m

The high yield parts of the aquiferous units in a typical basement terrain are principally located within the thick weathered or fractured overburden (otherwise known as saprolite zone) of the bedrock. The presence of fracture zones before the basement assists the groundwater potentials of the area by allowing easy seepage from neighboring aquifer/formation [28, 13]. This technique is bordered on high permeability that is readily available in a fractured basement. The fractured/fresh bedrock resistivity values delineated in the study area range from 660 – 6746  $\Omega$ m (Table 1). Therefore, a high yield of groundwater is expected to be found in VES1 and VES5 having the fractured basement with resistivity values of 660.2 and 972.3  $\Omega$ m respectively.

The inference drawn from the observation made from VES data showed that the second and third geo-electric layers are mainly contributory factors in identifying the rate of groundwater yield. All the sounding points in the study area demonstrated the same curve types (H-types). However, the deviations observed aid the cursory factor that determines the degree of groundwater yield in each sounding points. As a result of this, VES3 and VES4 will produce medium yield, while VES2, VES6, and VES7 will produce low yield. The classification is purely bordered on the estimated overburden thicknesses and the weathering conditions of the basement.

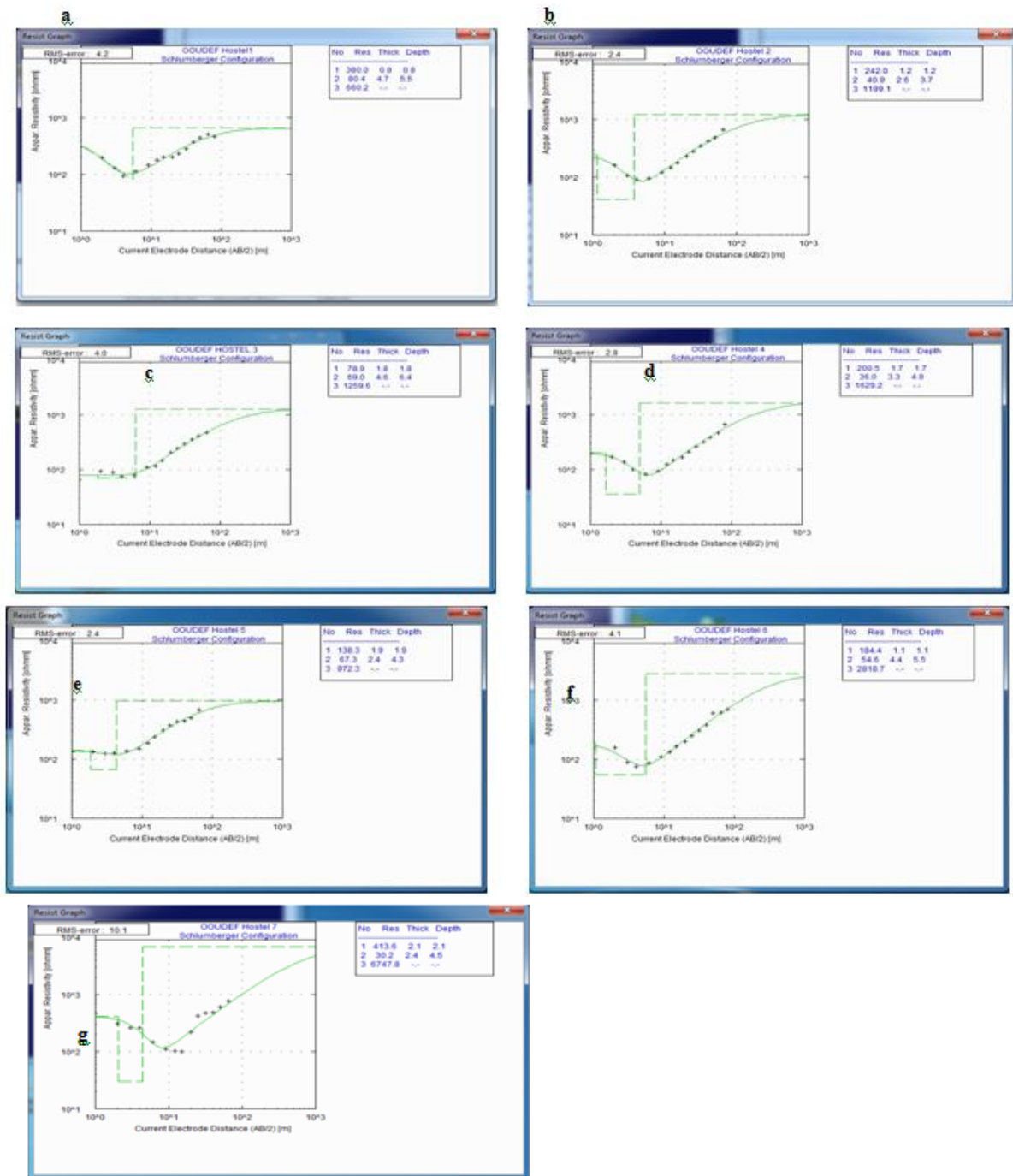


Figure 12: VES curve observed in the study area

### Isopach and Isoresistivity Map

The Isopach map illustrates the overburden thickness beneath the sounding points to demonstrate the thickness variation of each layer in the study area. The map inclines to give detailed information about the stratum that comprises the aquifer in the sounding point. The thickness and resistivity values of overburden are part of hydrogeologic parameters used in developing aquifer characteristics in basement terrain. This is because the water flows into the saturated zone through the overburden layers. The aquifer thickness map outlined in this study area disclosed that the southern and western parts of the study area exhibit the high value of thicknesses ranging from 4.0 – 4.6 m (Figure 13a). This is asymptomatic of aquifer of high yield.

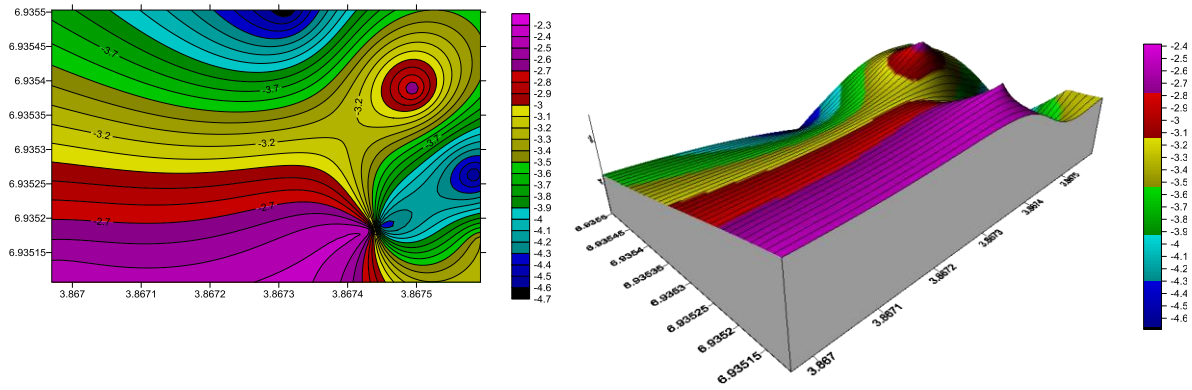


Figure 13a: Aquifer thickness map

Likewise, the overburden thickness map depicts that the deepest points are situated along with the eastern parts (Figure 13b). The iso-resistivity map was produced to different areas with low resistivity, which indicates the possibility of high water yield in the research area. The map shows the north and the eastern parts to have the highest resistivity values and the least found in the southwest and southeastern parts of the area of study as depicted in figure 13.

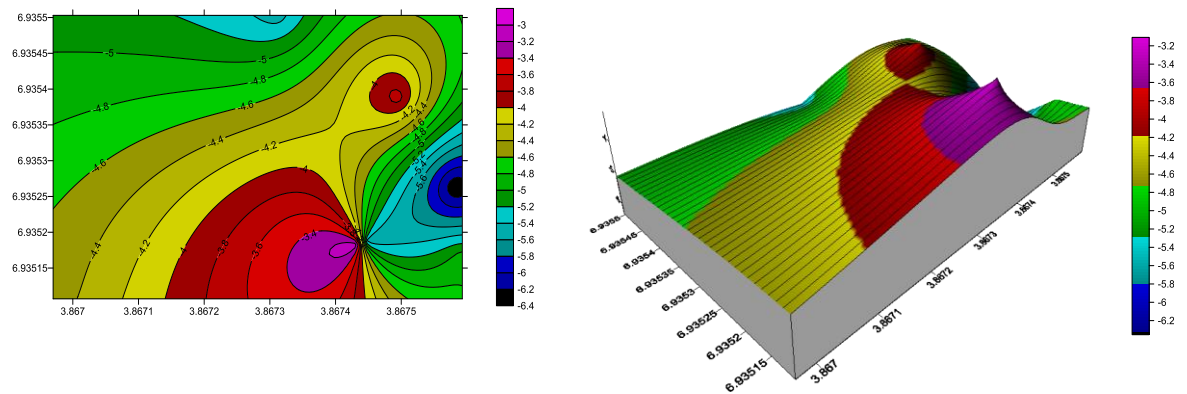


Figure 13b: Overburden thickness map

## V. Conclusions

The results of the electrical and magnetic methods have demonstrated the veracity of integrated methods in groundwater exploration. The integration of the two methods was found proficient enough to delineate the aquifer characteristics that border on the depth and its yield capacity. The magnetic method outlined the distribution of overburden thickness across the profile lines. Similarly, the aquifer thickness and its yield properties were estimated from the qualitative and quantitative analysis of the VES data. Although, H curve type ( $\rho_1 > \rho_2 < \rho_3$ ) are outlined for all the VES data in the study area they exhibit different lithological arrangement which bequeaths to their yield ratio. The Vertical Electrical Sounding (VES) results unraveled three layers of lithology whereas the second and third geo-electric layers described as the aquifer zone properties in the study area.

The integrated methods used affirmed that profile 1 will provide high groundwater yield having an overburden thickness of 6.3 and 7.4 as obtainable from VES and RMA respectively. The integration of these methods illustrated that the aquifer depths are within the depth values of 3.4 and 7.1 m across the sounding points. Therefore, the vertical electric sounding determines the layers and magnetic methods determine the magnetic intensity and gradient of the study area which are both helpful and useful for the exploration of groundwater. The integrated methods helped the study in providing the three (3) significant characteristics of an aquifer which are overburden thickness, weathered layer resistivity, and weathered/fractured basement resistivity.

## References

- [1]. Plummer, C.C., McGeary, D and Carlson, D.H. (1999). Physical Geology. 8th Edition, McGraw Hill Co. Inc., New York, 48-56
- [2]. Afolayan, J. F., Olorunfemi, M. O. &Afolabi, A. (2004). Geoelectric/Electromagnetic VLF survey for Groundwater development in a Basement terrain–A Case Study. *Ife Journal of Science*, 6(1), 74-78.
- [3]. Kumar, R., Musuuza, J. L., Van Loon, A. F., Teuling, A. J., Barthel, R., Ten Broek, J. &Attinger, S. (2016). Multiscale evaluation of the Standardized Precipitation Index as a groundwater drought indicator. *Hydrology and Earth System Sciences*, 20(3), 1117.
- [4]. Ochuko, U., and Thaddeus, O. (2013). Effect of underground on-site sewage disposal system on the quality of water from hand dug-wells in the urban center of Ughelli, Delta state Nigeria. *Standard Journal of Education and Essay*, 1(6), 81-90.
- [5]. OdoAra, H. T., Odunaike, R. K., Ogunsola, P. &Olaleye, O. A. (2013). Evaluation of groundwater potential using electrical resistivity method in the Okenugbo area, Ago-Iwoye, Southwestern, Nigeria. *International Journal of Engineering and Applied Sciences*, 4(5), 22-30.
- [6]. Adekoya, S. A., Coker, J. O., Oladunjoye, H. T. &Adenuga, O. A. (2019, August). Aquifer characterization of some parts of Ijebu Igbo using electrical resistivity methods. In *Journal of Physics: Conference Series* 1299 (1): 012075. IOP Publishing.
- [7]. Omosuyi, G.O., Ojo, J.S. &Enikanselu, P.A. (2003). Geophysical investigation for groundwater of Obanla-Obakekere in Akure Area within the Basement Complex of South Western Nigeria. *J Min Geol* 3(2):109 – 116
- [8]. Olasehinde, P.I. &Bayewu, O.O. (2011). Evaluation of Electrical resistivity anisotropy in geological mapping: a case study of OdoAra, west-central Nigeria. *Afr J Environ SciTechnol* 5(7):553–556
- [9]. Kayode, J. S. and Adelusi, A. O. (2010). Ground magnetic data interpretation of Ijebu - Jesa area, Southwestern Nigeria, using total component, *Research Journal of Applied Sciences, Engineering and Technology* 2(8):703 -709.
- [10]. Kayode, J. S., Nyabese, P. and Adelusi, A. O. (2010). Ground magnetic study of Ilesa East, Southwestern Nigeria, *African Journal of Environmental Science and Technology* 4(3):122 – 131.
- [11]. Umego, M. N. and Ojo, S. B. (1995). A magnetic depth to basement analysis in the Sokoto basin, Northwestern Nigeria, *Journal of Mining and Geology*, 31(2):161–167
- [12]. Akintayo, O. O. (2013). Geomagnetic and geoelectric investigation of mineral rocks at Awo, Osun State, Southwest Nigeria, *International Journal of Physical Research*, 1(2): 60– 74
- [13]. Mallam, A. (2004). Fresh basement: revealed from the resistivity method. *Zuma J Pure Appl Sci*. 6:6–9.
- [14]. Olorunfemi, M. O., Afolayan, J. F. and Afolabi, O. (2004). Geoelectric/electromagnetic VLF survey for groundwater in a Basement Terrain: a case study. *Ife J Sci* 6(1):74–78
- [15]. Olorunfemi, M. O. &Olorunniwo, M. A. (1985) Geoelectric parameter and aquifer characteristics of some parts of southwestern Nigeria. *GeolAppl E Hydrogeol* 2:99 – 109
- [16]. Kogbe, C. A. (1989). The Cretaceous and Paleogene Sediments of Southern Nigeria: In KogbeCa (Ed.), *Geology of Nigeria*. Elizabethan Publ. Lagos, Nigeria, pp 273-286.
- [17]. Rahaman, M. A. (1976). Review of the Basement Geology of Southwestern Nigeria, In *Geology of Nigeria*, C. A. Kogbe, Ed., pp. 41–58, Elizabethan. Lagos, Nigeria.
- [18]. Turner, D. C. (1983). Upper Proterozoic schist belts in the Nigerian sector of the Pan-African province of West Africa. *Precambrian Res.* 21(1–2):55–79.
- [19]. Ajibade, A. C., Woakes, M. and Rahaman, M. A. (1987). Proterozoic crustal development in the Pan-African regime of Nigeria. In: Kroner A, editor. *Proterozoic lithospheric evolution*. Washington DC (USA): American Geophysical Union; p. 259–271.
- [20]. Adelana, S. M. A., Olasehinde, P. I., Bale, R. B., Vrbka, P., Edet, A. E. &Goni, I. B. (2008). An overview of the geology and hydrogeology of Nigeria. *Applied groundwater studies in Africa*, 13, 171-197.
- [21]. Keary, P., Brooks, M. and Hill, I (2002). *An Introduction to Geophysical Exploration*. Third Edition, Blackwell Science Ltd. 168-183
- [22]. Trompat, H., Boschetti, F., & Hornby, P. (2003). Improved downward continuation of potential field data. *Exploration Geophysics*, 34(4):249-256.
- [23]. Foss, C. & McKenzie, B. (2011). Inversion of anomalies due to remanent magnetization: an example from the Black Hill Norite of South Australia. *Australian Journal of Earth Sciences*, 58(4), 391-405.
- [24]. Fairhead, J. D. and Williams, S. E. (2006). Evaluating normalized magnetic derivatives for structural mapping. In 2006 SEG Annual Meeting. Society of Exploration Geophysicists
- [25]. Olanikanmi, N., Bamigboye, O., Saminu, O., Salawu, N. and Bamidele, T. (2020). Interpretation of high-resolution aeromagnetic data of Kaoje and its environ, the western part of the Zuru Schist belt, Nigeria: implication for Fe–Mn occurrence. *Heliyon*, 6(1), e03320
- [26]. Thompson, D. T. (1982). EULDPH: A new technique for making computer-assisted depth estimates from magnetic data. *Geophysics*, 47(1):31-37.
- [27]. Olayinka, A. I. (1996): Non-uniqueness in the interpretation of bedrock resistivity from the sounding curve and its hydrological implications. *Water Resour J NAH* 7(1-2):55 – 60
- [28]. Aboh, H. O. and Osazuwa, I. B. (2000). Lithological deductions from a regional geoelectric investigation in Kaduna, Kaduna State Nigeria. *Niger J Phys*. 12:1–7.

Coker, J.O, et. al. "Groundwater Aquifer Delineation Within Some Parts Of Olabisi Onabanjo University, Southwestern Nigeria, Using Combined Electrical Resistivity And Magnetic Methods." *IOSR Journal of Applied Geology and Geophysics (IOSR-JAGG)*, 8(6), (2020): pp 17-28.